forests

Article

Does Tree Architectural Complexity Influence the Accuracy of Wood Volume Estimates of Single Young Trees by Terrestrial Laser Scanning?

Carsten Hess [1],*, Anne Bienert [2], Werner Härdtle [1] and Goddert von Oheimb [3]

[1] Faculty of Sustainability, Institute of Ecology, Leuphana University Lüneburg, Scharnhorststr.1, Lüneburg 21335, Germany; E-Mail: haerdtle@leuphana.de

[2] Institute of Photogrammetry and Remote Sensing, Technische Universität Dresden, Helmholtzstraße 10, Dresden 01069, Germany; E-Mail: anne.bienert@tu-dresden.de

[3] Institute of General Ecology and Environmental Protection, Technische Universität Dresden, Pienner Straße 7, Tharandt 01737, Germany; E-Mail: goddert_v_oheimb@tu-dresden.de

* Author to whom correspondence should be addressed; E-Mail: hess@leuphana.de; Tel.: +49-4131-677-2807; Fax: +49-4131-677-2808.

Abstract: Accurate estimates of the wood volume or biomass of individual trees have gained considerable importance in recent years. The accuracy of wood volume estimation by terrestrial laser scanning (TLS) point cloud data may differ between individual trees due to species-specific differences in tree architecture. We selected three common and ecologically important central European deciduous tree species, which differ considerably in tree architectural complexity in early ontogenetic stages: *Acer pseudoplatanus* (simple), *Sorbus aucuparia* (intermediate) and *Betula pendula* (complex). We scanned six single young trees for each species (18 trees in total) under optimal scan conditions (single tree stand, leafless state, four scanning positions, high resolution). TLS-based volume estimates were derived for the total tree as well as for the two compartments; trunk and branches, using a voxel-based bounding box method. These estimates were compared with highly accurate xyolmetric (water displacement) volume measurements. Coefficients of determination between xylometric measurements and bounding box estimates were very high for total trees ($R^2_{adj} = 0.99$), trunks ($R^2_{adj} = 0.99$), and high for branches ($R^2_{adj} = 0.78$). The accuracy of estimations for total tree and trunk volume was highly similar among the three tree species. In contrast, significant differences were found for branch volume

estimates: the accuracy was very high for *Sorbus aucuparia*, intermediate for *Betula pendula*, and low for *Acer pseudoplatanus*. A stepwise multiple regression showed that the accuracy of branch volume estimates was negatively related to the number of the first-order branches within diameter sizes of D ≤ 5 mm and crown surface area (R^2_{adj} = 0.61). We conclude that the accuracy in total tree and trunk volume estimates was not affected by the studied types of tree architectural complexity. The impact of the structural variability of branches and occlusion by branches was, thus, not as high as expected. In contrast, the accuracy of branch volume estimates was strongly influenced by tree architectural complexity, though not in a simple way. Because underestimations originated from different sources, the accuracy of branch volume estimates cannot be directly derived from the degree of architectural complexity. These results imply that the voxel-based bounding box method provides highly accurate total tree and trunk volume estimates, whereas further research is needed to improve branch volume estimation for young trees of different architectural types.

Keywords: bounding box; structural complexity; tree architecture; xylometric measurement; young trees

1. Introduction

In recent years it has become increasingly important to obtain accurate estimates of the wood volume or biomass of individual trees. These data are beneficial for multiple service forestries as a suitable forest management tool to produce a wide array of ecosystem goods and services such as timber and bioenergy production, carbon sequestration, and habitat provisioning [1].

In order to better manage multiple service forests, it is essential to improve the ability to predict their dynamics. In standard forest inventories, diameter at breast height (DBH) and tree height (TH) are measured manually, and tree volumes are calculated from these data using allometric equations [2]. For this allometric approach, the quality and quantity of the calibration data is crucial. In some regions the underlying data basis is very good for monospecific stands with even-aged trees, whereas forest stands that are structurally complex and diverse in species composition are much less well documented [3,4]. In these stands, individual trees display a large variation in shape and structure due to mixing effects, which may lead to substantial uncertainties when allometries obtained from uniform stands are applied [5,6]. Furthermore, allometric equations usually consider the trunk as the economically relevant aboveground woody component, but rarely branches. However, branch growth and development reflects tree growth responses to both biotic and abiotic environmental factors. Finally, the distribution of wood volume in the canopy cannot be calculated using allometric equations. Branch properties, tree crown structure, and canopy space filling are key characteristics in understanding light-use efficiency and tree-tree interactions [7,8], and thus the dynamics in multiple service forests. To obtain this information by direct field measurement is, however, challenging and time-consuming, and therefore costly [9].

In recent years, high-resolution inventory tools have been developed and are increasingly being used to acquire individual tree data. Of these, LiDAR (Light Detection And Ranging) and especially terrestrial laser scanning (TLS) have been applied to analyze standard tree dendrometrics such as stem position, tree density, DBH, TH, basal area, and wood volume [10–13]. For example, Hopkinson *et al.* [10] estimated DBH and TH based on TLS data, but still relied on standard allometric equations for wood volume estimates. Moreover, several authors [14–17] have developed and deployed methods to estimate wood volume based solely on TLS data.

These methods can be classified as voxel-based approaches and geometric model approaches. Voxel-based approaches address TLS points within a three dimensional (3D) voxel-grid. A voxel represents a cube with a unique position, edge length, and volume. If a voxel is occupied by points, the voxel will be used for volume estimation and wood volume is calculated by the summation of voxel volumes over all occupied (assigned) voxels [16,18,19], or is correlated with the total number of occupied voxels [14]. Because only the outer form or surface of an object can be obtained by TLS, the accuracy of this method will essentially increase by identifying and adding non-occupied, empty voxels inside the tree's structure. If these inner voxels are not included, they will not contribute to the total volume calculation, resulting in a substantial underestimation [18–20]. Alternatively, other approaches depend on geometric feature recognition within segments of the TLS points. Potentially representing a more natural model of the curved surface of the trunk and branches, cylinders are fitted within segments [21] and their volumes are summed for volume estimations [15,17,22–25].

The accuracy of the voxel-based approach is largely determined by the chosen voxel size [16,18]. A small voxel size will tend to underestimate volumes due to missing structural information. Larger voxel sizes will lead to an overestimation due to an increase of additional artificial cuboid structures around the natural surface of the tree. However, geometrical approaches also generate inaccuracies. Specific thresholds in the process of branch identification and in the reconstruction, especially of small branches, will lead to underestimations. Primarily depending on the experimental setting (scan resolution, scan positions, distances), the minimum diameters in branch detection and volume estimation range from 5 mm [26] over approximately 1 cm [27], 2 cm [22,28] and 4 cm [28] up to 7 cm [15].

All approaches have in common, however, that the accuracy of volume estimates depends on the primary quality of the point cloud representing the tree. Firstly, the scan resolution and the number of scan positions directly influences the point density and therefore the accuracy in capturing the structure of the (nearly complete) tree [29]. Secondly, post-processing of the point cloud by point cloud filtering to remove noise or ghost points may introduce inaccuracies if correct data points are wrongly removed. Thirdly, movements of target trees during the scan process as well as an imprecise registration process will lead to inaccuracies in the reconstruction of the tree structure and surface. In addition, fourthly, stand density and structural complexity, as well as the height of individual trees, directly influence the extent of occlusions and therefore the number of insufficiently captured structures within each scan.

The main objective of our study was to evaluate the accuracy of wood volume estimates as a function of the structural complexity of the scanned object. The structural complexity is different for different tree compartments (*i.e.*, the trunk and the branches), but also differs between tree species due to species-specific differences in tree architecture, predominantly characterized by the crown morphology and, thus, by the branch structures. Therefore, we separated the tree compartments' trunk and branches

and we selected three tree species that are very common and ecologically important in central Europe, but which differ considerably with regard to their architectural complexity: *Acer pseudoplatanus* (sycamore maple: simple), *Sorbus aucuparia* (rowan: intermediate), *Betula pendula* (European white birch: complex; these species are henceforth referred to as *Acer*, *Sorbus* and *Betula*). In order to keep all other influencing factors constant, we used an experimental setting under ideal field conditions with uniform scan data acquisition and post-processing procedures. We selected young trees because the differences in tree architecture are most significant in young and middle-aged stands [8] and because the relative proportion of small branches to the total tree volume is highest.

For our study, we used a voxel-based approach in combination with a bounding box method for outer voxels, as published by Bienert *et al.* [16]. Compared to simple voxels (cubes) the bounding box method offers a closer fit of adapted cuboid bodies (bounding boxes) at the surface of the tree to reduce overestimations and to fully reveal species-dependent amounts of structural gaps due to occlusions. The accuracy of voxel-based volume estimates was validated against direct xylometric measurements. To our knowledge, this is the first study to analyze the accuracy of voxel-based volume estimates for different tree compartments of species with different tree architectural complexity. Specifically, we hypothesized that:

(H1) Volume estimates for trunks are more precise than those for branches due to differences in size, orientation and extent of occlusion.

(H2) Accuracy of volume estimation decreases in the order *Acer* > *Sorbus* > *Betula* due to differences in tree architectural complexity (low: *Acer*, high: *Betula*) and the extent of occlusions by branches (low: *Acer*, high: *Betula*).

2. Methods

2.1. Study Site and Target Trees

The study site Enzen forest is located near Stadthagen in the lowlands of Lower Saxony (52° 19.279 N, 9° 9.851 E, altitude 80 m above sea level). The climate is sub-Atlantic with a mean annual precipitation of 723 mm and a mean annual temperature of 8.9 °C. The dominant soil type is Pseudogley-Parabraunerde. The current forest vegetation is meso- to eutrophic sub-Atlantic oak-hornbeam mixed forest (Stellario-Carpinetum; NATURA 2000 Code: 9160).

The forest stand used for this study covers an area of about 5 ha. The overstory is dominated by the tree species *Quercus robur*, *Carpinus betulus*, *Fagus sylvatica*, *Larix decidua* and *Acer*. The understory is very species-rich, with all overstory tree species being present (except for *Quercus robur*), as well as other species, consisting primarily of *Betula*, *Sorbus*, *Taxus baccata*, *Prunus avium*, *Fraxinus excelsior*, *Corylus avellana*, *Crataegus* spec. and *Ilex aquifolium*. The overstory had a mean basal area of 20.0 m^2 ha^{-1} and a mean density of 110 stems ha^{-1}. The mean density of the understory was 2500 stems ha^{-1}, and the maximum tree height was about 8 m.

We selected six individual young trees from each of the three species *Acer*, *Sorbus* and *Betula i.e.*, a total of 18 target trees. The selection criteria were: only understory trees, and tree height within the range of five to eight meters. The target trees were located in one group each in the case of *Acer* and *Betula* (patch size about 8 m^2 each), and in two distinct groups in the case of *Sorbus* (patch size about

3 m^2 each). Table 1 gives a descriptive overview of the 18 target trees. Tree age was analyzed by counting the tree rings of stem discs from the stem base under a binocular microscope. Diameter at the stem base (ground diameter, GD) and DBH were measured with a diameter tape at 0.1 cm intervals. TH was measured with a measuring tape as the length of the chopped trunk.

Table 1. Descriptive statistics for the 18 target trees: tree age (Age), ground diameter (GD), diameter at breast height (DBH) and total tree height (TH).

Species	No	Age (year)	GD (cm)	DBH (cm)	TH (m)
Acer	1	15	4.2	2.8	5.28
	2	14	3.8	2.8	5.70
	3	16	3.8	3.2	6.75
	4	16	4.0	3.0	5.93
	5	14	4.4	3.5	6.50
	6	16	3.6	2.5	5.52
mean		*15.2*	*4.0*	*3.0*	*5.95*
Sorbus	1	12	5.2	4.5	7.96
	2	12	5.0	4.3	6.80
	3	12	4.8	3.9	6.27
	4	11	5.0	4.0	6.92
	5	11	4.0	3.3	7.50
	6	11	3.5	2.9	7.02
mean		*11.5*	*4.6*	*3.8*	*7.08*
Betula	1	10	5.3	3.6	6.68
	2	10	6.3	4.5	7.35
	3	10	3.8	3.1	6.76
	4	10	6.5	4.6	6.99
	5	10	4.7	3.5	5.76
	6	10	3.8	2.8	6.53
mean		*10.0*	*5.1*	*3.7*	*6.68*

The age range of the target trees was 10 to 16 years, with *Betula* having the lowest mean age (10.0 years) and *Acer* having the highest mean age (15.2 years; *Sorbus*: 11.5 years). The GD and DBH ranges were 3.5 to 5.2 cm and 2.5 to 4.6 cm, respectively, and tree heights varied between 5.3 and 8.0 m. *Acer* had both the lowest mean GD and the lowest TH, whereas these mean values were very similar for *Betula* and *Sorbus*.

2.2. Scan Data Acquisition

All data was recorded within two days in December 2013 under leaf-off conditions for the deciduous trees and nearly windless conditions. The scans were performed with a phase-shift FARO Laser Scanner Photon 120 (FARO Technologies Inc., Lake Mary, FL, USA). Details of technical specifications and experimental settings for the scan procedure are presented in Table 2.

Table 2. Technical specification and experimental settings of the FARO LS Photon 120.

FARO LS Photon 120	Hardware Specifications	Experimental Settings
Measurement range	0.6–120 m	
Ranging error	±2 mm (at 10 m)	
Beam diameter	3 mm at exit, 4 mm at 3 m	
Field-of-view (V × H)	Up to 310° × 360°	310° × 70°
Angular step size (V, H)	Up to 0.009°	0.036°
Spatial resolution	Up to 2 mm (at 15 m)	1.9/2.5/3.1/3.8 mm (at 3/4/5/6 m)
Data acquisition rate (X-Control)	Up to 976,000 points/sec.	244,000 points/sec. (3×)
Scan time		1:50 min
Filter *Clear-Sky*/*Clear-Contour*		active/active
Instrument height		1.3 m
Number of scanning positions		4
Distance between laser scan positions and mounted tree		3 m

Our aim was to conduct the scanning under field conditions (*i.e.*, existence of a tree overstory, ambient temperature, humidity, and air movements), but at the same time to strictly control the conditions of the scanning procedure with regard to: (i) avoidance of any occlusion of the target trees by neighboring trees or ground vegetation; (ii) standardized set-up of the position of the laser scanner and the scan tie points (registration spheres). To achieve these aims each target tree was sawn off with a hand saw at ground level, transported over a distance of about 20 m to a forest patch with widely spaced overstory trees and missing understory, and fixed in a tree stand. The laser scanner was positioned on a tripod at a height of 1.3 m. Each isolated tree was scanned from four fixed positions (perpendicular to each other) at a distance of 3.0 m from the trunk. For the registration process four polystyrene spheres (radius: 14.5 cm) each were placed inside and outside the scan area, respectively (Figure 1).

Figure 1. Tree no. 1 of *Betula* mounted on a stand. The four reference spheres inside the scan area can be clearly seen in the foreground, and one of the four reference spheres outside the scan area is visible behind the trunk.

2.3. Scan Data Registration and Post-Processing

During the scan process, FARO LS built-in hardware filters *Clear-Contour* and *Clear-Sky* were applied to the recorded data. The filter *Clear-Contour* removed incorrect measurements when a laser beam was reflected twice when hitting two different surfaces. The filter *Clear-Sky* removed incorrect point results when scanning the sky and did not hit any scan object at all [30].

For each tree, raw scan data from all four scan positions were registered in the FARO LS associated software FARO Scene (FARO Technologies Inc., Version 5.0.1, Lake Mary, FL, USA, 2012). Before registration a predefined standard filter for point cloud optimization was applied for each individual scan. This standard filter algorithm is based on specific stray point filtering in combination with a minimal threshold in intensity of the reflected laser pulse. Registration was performed automatically by FARO Scene using the reference spheres. With the registration process, the point clouds obtained by the four laser scanner positions were transformed into a common project coordinate system.

From the registered point cloud data, each tree was extracted manually as a single tree point cloud (Figure 2) using the software CloudCompare (CloudCompare, Version 2.5.4, Paris, France, 2014). A copy of the tree's point cloud was additionally split into two separate point clouds consisting of the trunk, and all the branches, respectively. Each of these point cloud objects (*i.e.*, total tree, trunk and branches) was post-processed by a statistical outlier remover filter plugin (qPCL) within CloudCompare to remove residual noise and ghost points. The cleaning filter analyzes 10 neighboring points and their distances. Points with a distance larger than one standard deviation plus the mean distance to the query point are marked as outliers and removed.
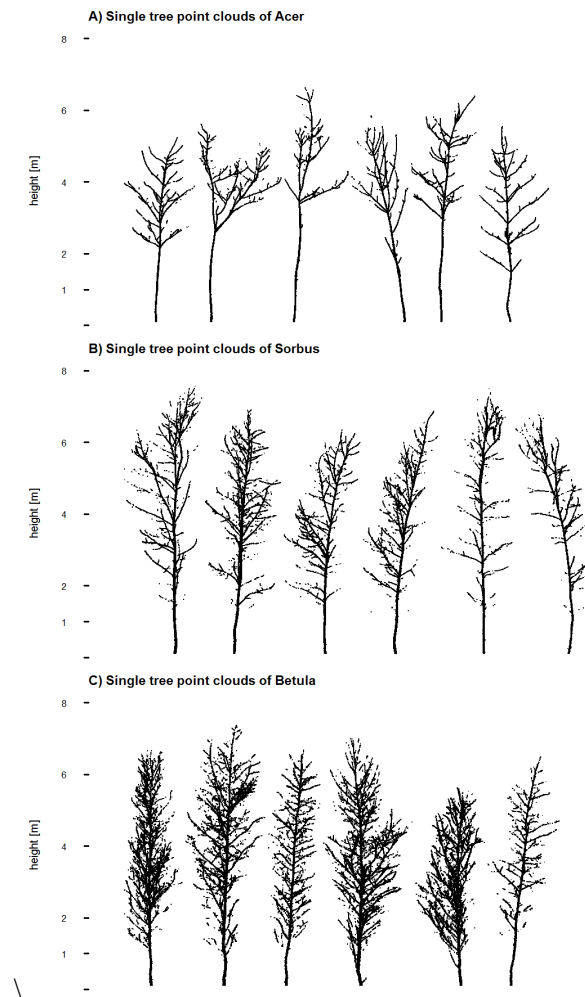
Figure 2. 2D images of all filtered single tree point clouds for (**A**) *Acer*; (**B**) *Sorbus* and (**C**) *Betula*.

2.4. Architectural Complexity—Tree Characteristics

Different measurements and analyses of branch and crown variables were carried out on the target trees to quantify differences in the architectural complexity between the tree species in detail.

For the determination of branch variables and for the xylometric measurements (see below) the target trees were destructively divided into different compartments directly after the scan process. The first division was into trunk and branches. At branch level we differentiated between branch orders. The first branching away from the main axis is the first-order branch. The branching from the first-order branch results in a second-order branch, and so forth. For all branches and all order levels the length (BLen, in cm) and the diameter at branch center (BDia, in mm) were measured.

Depending on the branch order level all branches were categorized into either diameter classes (first-order branches) or length classes (all higher-order branches). The first-order branches were assigned to three classes with a diameter (D) at branch collar of $D \leq 5$ mm (D5), 5 mm $< D \leq 10$ mm (D10) and $D > 10$ mm (D10+). Higher-order branches were categorized in three length (L) classes with $L \leq 20$ cm (L20), 20 cm $< L \leq 40$ cm (L40) and $L > 40$ cm (L40+). The number of branches (BNum) was counted for each diameter class (first-order branches) and each length class (all higher-order branches).

Based on the point clouds, four crown-related structural complexity variables were also calculated. These were: Crown height (CH) as the difference in height along the Z-axis between the starting point of the lowest first-order branch and the highest tree point; crown volume (CV) as the volume of a 3D convex hull of the crown; crown surface area (CSA) as the surface area of the 3D convex hull of the crown; and crown projection area (CPA) as the area of the 2D convex hull of all crown points projected in the xy-plane.

2.5. Volume Estimations

2.5.1. Xylometric Measurements

For the xylometric measurements all trunks were cut into sections of 65 cm in length so that they fit into the water container. Branches were measured in bundles of classes consisting of the branch order levels first-order branches or higher-order branches. Each trunk segment or branch bundle was fully submerged in a specifically constructed cylindrical water container (Figure 3). The displaced and collected water was weighted and the equivalent water volume was calculated and assigned to each compartment. The xylometric volumes were determined directly after the scan process so that no reduction in wood volume should have occurred. As the period of submergence of each object was very short, the impact of water permeation into the wood was negligible.

Figure 3. Medium-sized xylometer with a diameter of about 12 cm and overflow height of about 90 cm.

2.5.2. Voxel-Based Analyses

Volume estimates from the point clouds of total tree, trunk, and branches were obtained by an extended version of the voxel-based method published by Bienert *et al.* [16]. All points from the filtered point cloud data are allocated to their individual voxel within the defined voxel-grid of 5 mm. Based on these occupied voxels, non-occupied empty voxel inside larger tree segments (shadow voxels) are identified similar to the method of Hosoi *et al.* [19]. To minimize overestimations the

volume of the outer hull voxels is adjusted to the actual point distribution within each voxel by a determined axis-parallel bounding box. To close gaps between all neighboring bounding boxes and inner shadow voxels, the bounding boxes have to be expanded to the border of a neighboring shadow or bounding box voxel. This method provided two vital advantages: (1) the consideration of empty voxels inside tree structures (especially inside the trunk) for volume estimations and (2) a reduction of overestimation due to a closer outer surface fit thanks to the creation of smaller bounding boxes within each voxel.

To compare the influence of species-specific architectural complexity to the accuracy of volume estimations, all point clouds were processed with the same voxel size. At a distance of three meters, the spatial scan resolution was 1.9 mm (Table 2). At an overall mean tree height of about 6.6 m and a scanner height of 1.3 m we assumed a maximum distance between the laser scanner and branches at the top of the trees of about five to six meters. At a distance of six meters, the spatial scan resolution was 3.8 mm. In order to enclose at least two neighboring measurement points within one voxel we chose a voxel size of 5 mm. As most branches had a diameter at branch collar of less than 10 mm, a voxel size of 5 mm will probably not create many empty voxels inside branch structures. With the close fit of the bounding boxes to the surface of the point cloud structures, we expected an underestimation in volume estimations due to missing structural information caused by occupations or the filter algorithm.

2.6. Data Analyses

We tested for significant differences in architectural complexity variables between the tree species using one-way ANOVA. To test our hypotheses we assumed a linear relationship between volumes estimated by TLS and xylometric measurements. For each point cloud (total tree, trunk, and branches) we calculated adjusted R^2 (R^2_{adj}) values of a linear regression for all species and for each species separately. The differences in volume determination from xylometric measurements and from voxel-based estimations were expressed as absolute and relative differences. One-way ANOVA was used to test for relative differences in volume estimates among tree species. In order to investigate the influence of architectural complexity variables on the relative differences in volume estimates, a stepwise multiple regression was performed for every point cloud (total tree, trunk, and branches). All statistical analyses were performed using the software R [31].

3. Results

3.1. Architectural Complexity

The three species differed significantly in all branch variables (Figures 4 and 5) and in three out of four crown variables (CH, CV, CSA; Figure 6). Generally, *Acer* showed the lowest, and *Betula* the highest values in the number of branches and total branch lengths. For example, the means for total number of branches were 108 in *Acer* and 977 in *Betula* (214 in *Sorbus*; ANOVA: $p < 0.001$). The overall sum of the mean total length of all branches amounted to 29.2 m in *Acer*, to 81.0 m in *Sorbus* and to 239.2 m in *Betula* (ANOVA: $p < 0.001$).
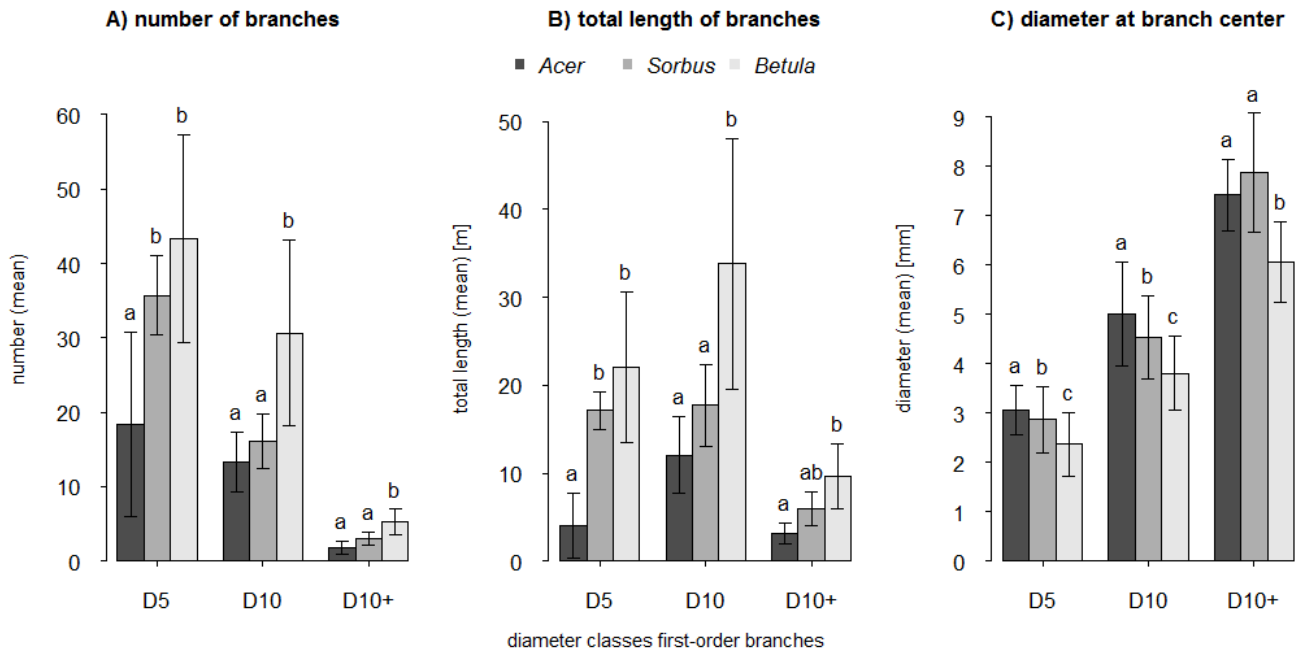
Figure 4. Barplots of mean values (and SD) of the structural complexity variables (**A**) branch number, (**B**) total length of branches and (**C**) diameter at branch center for first-order branches and diameter classes: D5 ≤ 5 mm, 5 mm < D10 ≤ 10 mm, D10+ > 10 mm. Different lower case letters indicate significant differences between tree species in *post hoc* Tukey tests ($p < 0.05$).
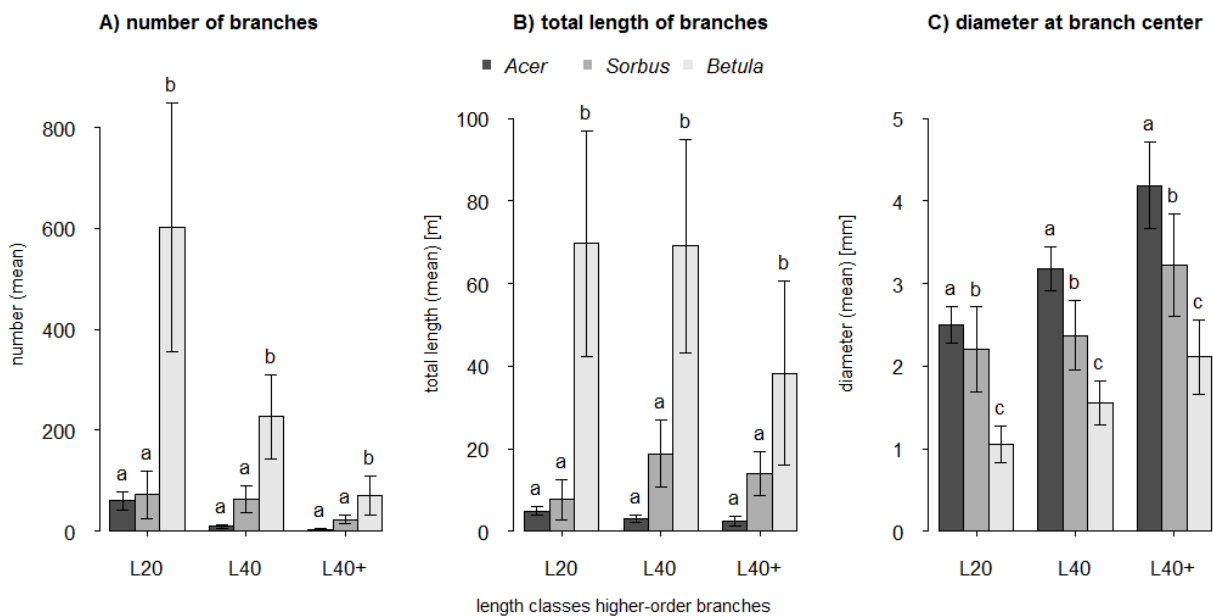
Figure 5. Barplots of mean values (and SD) of the structural complexity variables (**A**) branch number, (**B**) total length of branches and (**C**) diameter at branch center for higher-order branches and length classes: L20 ≤ 20 cm, 20 cm < L40 ≤ 40 cm, L40+ > 40 cm. Different lower case letters indicate significant differences between tree species in *post hoc* Tukey tests ($p < 0.05$).
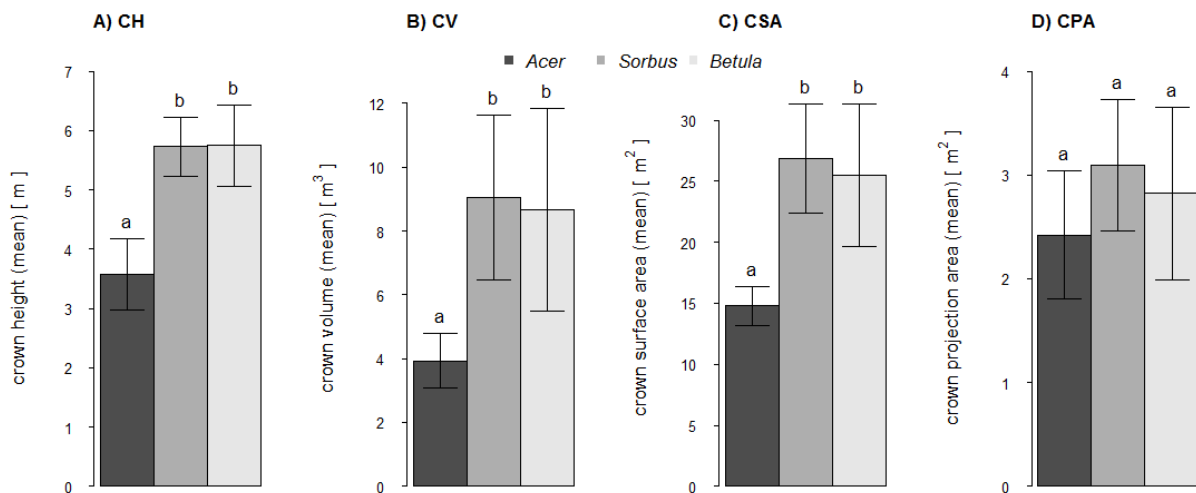
Figure 6. Barplots of mean values (and SD) of the crown variables (**A**) crown height (CH), (**B**) crown volume (CV), (**C**) crown surface area (CSA) and (**D**) crown projection area (CPA). Different lower case letters indicate significant differences between tree species in *post hoc* Tukey tests ($p < 0.05$).

In the first-order branches, *Acer* always had significantly lower numbers and total lengths than *Betula*, whereas some of the *Sorbus* values were more similar to those of *Acer* (e.g., number of branches in D10 and D10+) and partly more similar to those of *Betula* (e.g., number of branches in D5, Figure 4A,B).

The numbers and total lengths of the higher-order branches were always significantly lower in *Acer* and *Sorbus* than in *Betula* (Figure 5A,B). In addition, the differences between the species were much more distinct than in first-order branches. For example, the mean number of branches of *Betula* in the length class L20 was ten and eight times higher than in *Acer* and *Sorbus*, respectively, and in the length classes L40 and L40+ the values were extremely low for *Acer* (10 and 4, respectively, compared to 64 and 24 in *Sorbus* and 227 and 71 in *Betula*). In contrast, branch diameters showed the opposite pattern: *Acer* always had significantly higher values than *Betula* (Figures 4C and 5C). With one exception (branch diameter in D10+), *Sorbus* took an intermediate position.

Finally, *Acer* had significantly lower CH, CV, CSA than *Sorbus* and *Betula* (Figure 6A–C), whereas the latter two did not differ significantly from one another with regard to these crown variables. CPA showed no significant differences between the three species (Figure 6D).

3.2. Xylometric Measurements

The xylometric measurements revealed that the total tree volume of *Sorbus* and *Betula* was almost twice the total tree volume of *Acer* (Table 3). The same pattern was observed for the volumes of the trunk and branches. The mean proportion of the branch volume from the total volume was lowest in *Acer* (19%) and highest in *Betula* (25%; *Sorbus* 21%). With a mean value of 82%, the first-order branches of *Acer* had the highest proportion of the total branch volume, followed by *Sorbus* (71%) and *Betula* (63%).

Table 3. Xylometric volume measurements (V$_{Xylo}$) and bounding box volume estimates (V$_{BBox}$) for each tree and point cloud (total tree, trunk and branches), resulting absolute (Δ abs. = V$_{BBox}$ − V$_{Xylo}$) and relative differences (Δ rel. = (V$_{BBox}$ − V$_{Xylo}$) / V$_{Xylo}$ × 100) and their mean values. Different lower case letters indicate significant differences between tree species in *post hoc* Tukey tests ($p < 0.05$).

Species	No.	Total Tree					Trunk					Branches				
		V$_{Xylo}$ [dm³]	V$_{BBox}$ [dm³]	Δ abs. [dm³]	Δ rel. [%]		V$_{Xylo}$ [dm³]	V$_{BBox}$ [dm³]	Δ abs. [dm³]	Δ rel. [%]		V$_{Xylo}$ [dm³]	V$_{BBox}$ [dm³]	Δ abs. [dm³]	Δ rel. [%]	
Acer	1	2.849	2.203	−0.646	−22.7		2.173	1.632	−0.541	−24.9		0.676	0.530	−0.147	−21.7	
	2	3.489	2.718	−0.771	−22.1		2.819	2.193	−0.627	−22.2		0.670	0.463	−0.207	−30.9	
	3	3.673	2.708	−0.965	−26.3		3.181	2.307	−0.874	−27.5		0.492	0.362	−0.130	−26.5	
	4	3.459	2.672	−0.787	−22.7	a	2.736	2.039	−0.697	−25.5	a	0.722	0.576	−0.147	−20.3	a
	5	4.566	3.252	−1.314	−28.8		3.858	2.674	−1.183	−30.7		0.708	0.535	−0.173	−24.5	
	6	2.324	1.923	−0.402	−17.3		1.847	1.381	−0.466	−25.3		0.477	0.527	0.050	10.4	
mean		*3.393*	*2.579*	*−0.814*	*−23.3*		*2.769*	*2.038*	*−0.731*	*−26.0*		*0.624*	*0.499*	*−0.126*	*−18.9*	
Sorbus	1	8.522	6.633	−1.888	−22.2		6.790	5.478	−1.312	−19.3		1.732	0.951	−0.780	−45.1	
	2	7.575	5.847	−1.728	−22.8		5.620	4.516	−1.103	−19.6		1.955	1.028	−0.928	−47.4	
	3	5.260	4.270	−0.990	−18.8		4.183	3.449	−0.734	−17.6		1.077	0.695	−0.382	−35.5	
	4	6.524	4.954	−1.570	−24.1	a	5.118	4.084	−1.034	−20.2	a	1.407	0.685	−0.721	−51.3	b
	5	4.667	3.601	−1.067	−22.9		3.819	3.105	−0.714	−18.7		0.848	0.426	−0.422	−49.8	
	6	3.675	2.680	−0.995	−27.1		2.968	2.241	−0.727	−24.5		0.707	0.344	−0.363	−51.3	
mean		*6.037*	*4.664*	*−1.373*	*−23.0*		*4.749*	*3.812*	*−0.937*	*−20.0*		*1.288*	*0.688*	*−0.599*	*−46.7*	
Betula	1	5.787	4.370	−1.417	−24.5		4.168	3.043	−1.126	−27.0		1.619	1.148	−0.470	−29.1	
	2	8.513	6.629	−1.884	−22.1		6.633	5.410	−1.223	−18.4		1.880	0.855	−1.025	−54.5	
	3	3.841	2.617	−1.224	−31.9		3.045	2.144	−0.902	−29.6		0.795	0.302	−0.493	−62.0	
	4	9.801	7.492	−2.309	−23.6	a	6.708	5.640	−1.068	−15.9	a	3.093	1.486	−1.607	−52.0	b
	5	4.742	3.748	−0.994	−21.0		3.286	2.286	−1.000	−30.4		1.456	1.263	−0.192	−13.2	
	6	3.005	2.179	−0.825	−27.5		2.523	1.917	−0.606	−24.0		0.481	0.191	−0.290	−60.3	
mean		*5.948*	*4.506*	*−1.442*	*−25.1*		*4.394*	*3.407*	*−0.988*	*−24.2*		*1.554*	*0.874*	*−0.680*	*−45.2*	

3.3. Voxel-Based Volume Estimations

Overall, the coefficient of determination between xylometric measurements and voxel-based estimates was very high for the total trees (R^2_{adj} = 0.993; Figure 7A). However, these values differed between trunks and branches. Whereas it was also very high for trunks, it was high for branches (R^2_{adj} = 0.988 and R^2_{adj} = 0.780, respectively; Figure 7B,C).
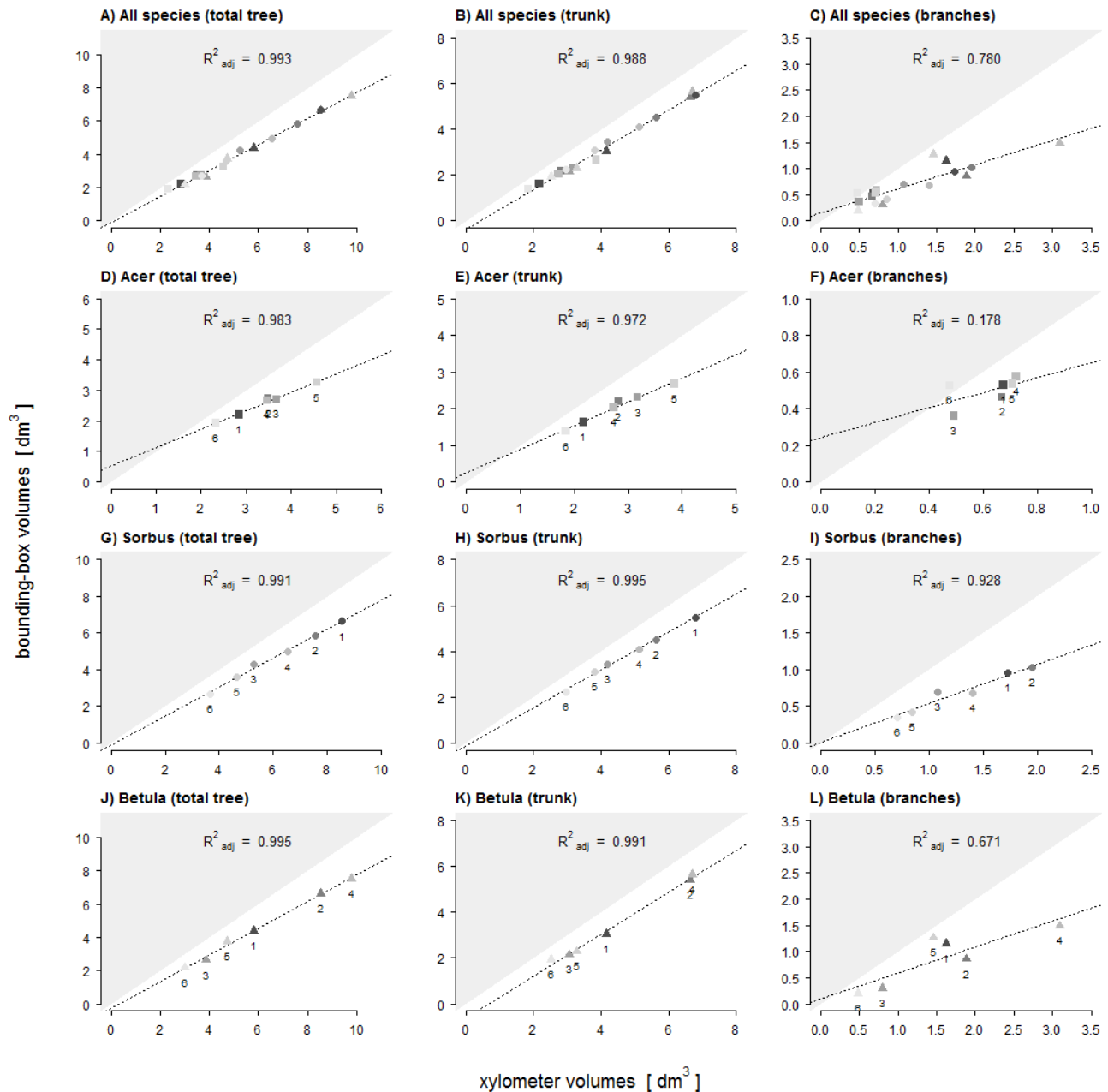
Figure 7. Regression plots of xylometric and bounding box volumes with determined R^2_{adj} values for the total tree, trunk and branches of all trees (**A**–**C**), *Acer* (**D**–**F**), *Sorbus* (**G**–**I**) and *Betula* (**J**–**L**). 1:1 line is visualized by the borderline of the grey triangle.

The accuracy of estimation for total tree volume was highly similar among the three tree species with the rank order *Acer < Sorbus < Betula* (*Acer* R^2_{adj} = 0.983; *Sorbus* R^2_{adj} = 0.991; *Betula* R^2_{adj} = 0.995; Figure 7D,G,J).

Likewise, very similar R^2_{adj} values were found for the accuracy of trunk volume estimation (*Acer* R^2_{adj} = 0.972; *Sorbus* R^2_{adj} = 0.995; *Betula* R^2_{adj} = 0.991; Figure 7E,H,K).

In contrast, large differences were found for the coefficients of determination for the branches: the accuracy was very high for *Sorbus* (R^2_{adj} = 0.928) and intermediate for *Betula* (R^2_{adj} = 0.671). By far the lowest value was observed for *Acer* (R^2_{adj} = 0.179; Figure 7F,I,L).

Relative differences in bounding box derived estimates of the total tree volume were very similar between the three species, showing an underestimation with mean values ranging from −23.0% to −25.1% (Table 3). Likewise, mean relative differences in trunk volume estimates did not differ significantly among the species (mean underestimation of −20.0% to −26.0%). In contrast, mean relative differences in branch volume estimates were significantly smaller in *Acer* (−18.9%) than in *Sorbus* and *Betula* (−46.7% and −45.2%, respectively; Table 3). As a result, the underestimation of volumes was in the same order of magnitude for the total tree, as well as for the two compartments (trunk and branches) in *Acer*, whereas it was considerably higher for branches than for total tree and trunk in *Sorbus* and *Betula*.

Multiple regression analysis revealed that the relative differences in bounding box derived estimates of the total tree volume could not be explained by any structural complexity variable (Table 4). Relative differences in trunk volume estimates were significantly positively related to CV (R^2_{adj} = 0.389). This indicates that the relative differences in trunk volume estimates decreased for trees with increasing CV. Relative differences in branch volume estimates were negatively related to the number of first-order branches of the diameter class D5 and the CSA (R^2_{adj} = 0.610).

Table 4. Final results of the stepwise multiple regression models with relative difference of volume estimates (Δ rel. = (V_{BBox} − V_{Xylo}) / V_{Xylo} × 100) as the dependent variable and most significant structural complexity variables as predictor variables for all point clouds of the total tree, trunk and branches. Abbreviations: CV: crown volume; BNum (D5): number of first-order branches in the diameter class D ≤ 5 mm; CSA: crown surface area. Beta values represent the standardized regression coefficients.

Model for	Predictor	Std. Est.	Std. Err.	F	*t*	*P*	R^2_{adj}	Beta
total tree		no significant single predictor variable						
trunk	(Intercept)	−29.98	2.09	11.82	−14.32	<0.001	0.39	
	CV	0.91	0.26		3.44	0.0034		0.65
branches	(Intercept)	12.16	10.30	14.32	1.18	0.2565	0.61	
	BNum (D5)	−0.72	0.20		−3.58	0.0028		−0.57
	CSA	−1.15	0.44		−2.59	0.0205		−0.42

4. Discussion

Overall, the extended voxel-based algorithm with bounding boxes provided highly congruent volume estimates based on TLS point clouds when compared to the direct volume determination. Results attested that we used a reliable method for wood volume estimation. As assumed, the chosen voxel-size of 5 mm generated underestimations for all tree point clouds.

In our study, we experimentally excluded the occlusion of the target tree by external structures and standardized scan positions for data recording. In addition, we tried to control wind impact by scanning under nearly windless conditions. Nevertheless, visual inspection of the tree point clouds revealed some significant structural inaccuracies within the crown, probably due to global registration errors which affect volume estimates by locally expanding tree segments. Ultimately, we identified two possible reasons. Although we placed a total of eight reference spheres (four inner and four outer spheres) around each target tree, we could only use up to four spheres to register the scans. To achieve a shorter scan duration we reduced the scanner's horizontal field-of-view to 70° (*cf.* Table 2) and therefore only the inner four spheres and one outer sphere on the opposite site of the scanner were captured within each scan. Additionally, the spheres were positioned mainly near the ground. A larger variation in distances and vertical positioning among the spheres would probably have helped to reduce registration errors. To enhance the quality of globally registered tree stands, Bucksch and Khoshelham [32] presented a skeleton-based re-registration routine applied to point cloud data of single scans to optimize registration of segments such as branches of individual trees. A comparable approach but on stand level was presented by Bienert and Maas [33] who used the vertical axis of scanned trees to enhance registration quality.

Furthermore, voxels occupied by noise or ghost points originating from measurement errors would lead to overestimations [16]. Point cloud filter could remove a large proportion of these measurement errors, but most likely there will always be a loss of structural information. If correct measurement points from insufficiently recorded parts of the tree are removed, the amount of underestimation could increase, especially when the fraction of small branches is high. When working with imperfect and unorganized raw point cloud data (without topological information on the trunk and branches), a filter algorithm is needed which prevents branch structures with low point densities from being removed. Although subjective and individual quality control in point cloud filtering is beneficial in preserving branch structures from being removed [17,28], processing hundreds of trees requires automated filtering processes. Skeletonization of raw point clouds and resultant topological tree models could preserve structural information and prevent low point densities from being removed or could even add structural information by closing gaps between disconnected branch segments [22].

Finally, regarding the size of relative differences between real volume (derived by xylometric measurements) and bounding box volume estimations, the accuracy strongly depends on the selected voxel size. To reveal all kinds of structural inaccuracies during the scan process or rather to identify missing structural information due to occlusions, low point densities and point cloud filter, we applied a small voxel size to realize a bounding box model with a close fit to the surface of the TLS point cloud. From this initial small voxel size, increasing the voxel size will counteract underestimations by overestimation as larger bounding boxes add additional volumes with no corresponding structures of TLS points. A tipping point would be reached when underestimations are balanced by overestimations.

Finding this individual tree-specific tipping point as determined by an individual voxel size seemed impossible, or at best barely feasible and will add a new source of inaccuracy.

As predicted by H1 we found that trunk volume estimates were more accurate than branch volume estimates. Trunks not only have larger diameters than branches, but they also differ in their main growth orientation. We assume that both issues contribute to more precise scan results for trunks compared to branches. Structures with a greater surface area will be better captured even with comparatively low scan resolutions. The vertical growth orientation of the trunks enabled an all-around scanning of the whole structure. The extent of occlusions in higher trunk fractions is small compared to that of inclined or horizontal branches located far above the laser scanner. Nevertheless, there will be blind spots inside a branch fork when branches are orientated in line with the trunk and laser beam. Also the relation between voxel-size and diameter of the trunk or branch segment affects the possible accuracy of the volume estimation. A larger diameter results in a shallower circular arc and a better fit of the cuboid lateral plane to the curved area of the surface. Multiple regression analysis showed that the relative differences (underestimations) of trunk volume estimates significantly decreased with increasing crown volume (CV: R^2_{adj} = 0.39). A larger crown volume indicates a larger tree size with a larger and better captured trunk. The relative differences of volume estimates for branches seemed to be primarily dependent on the number of first-order branches of the smallest diameter class D5 (≤5 mm) and the surface area of the crown (BNum (D5) + CSA: R^2_{adj} = 0.61). Compared to higher-order branches, first-order branches account for a relatively high fraction of total tree volume (~15%). However, first-order branches within the diameter class D5 are less well captured than larger first-order branches (D10, D10+). Branches with a diameter close to or smaller than the scan resolution are only captured and represented by a few points or even only by a line of single points. This also applies to the higher-order branches with even smaller diameters whose influence might be expressed by the crown surface area as the predictor variable. These branches contribute to a higher level of underestimation, certainly amplified after applying the point cloud filter.

With regard to total tree and trunk volume estimates, we could not confirm H2 because only very small (and not significant) differences between the three tree species were found. For total tree volume estimates all tree species showed very high R^2_{adj} values (>0.98; Figure 7D,G and J). As mean values of relative differences only differed within the small range of 2.1% we could not determine a clear accuracy ranking between the three species. Our results suggest that fewer but larger branches might lead to a similar or even greater extent of occlusions than a very high number of smaller branches. From the point of view of scan position, occlusions of the trunk by branches will be high if branch and trunk are congruent in their spatial growth orientation and also increases with increasing branch diameter. A second reason might be greater open contours on the trunk surface of *Acer* after the segmentation of all branches within the point clouds. The larger the sizes and proportion of open contours on the trunk surface the more empty voxels there are inside the trunk which will not be identified and considered as trunk volume.

The accuracy of branch volume estimates for *Acer* differs significantly from *Sorbus* and *Betula*. As volume estimates of *Acer* showed the lowest congruence, the accuracy ranking for the branches was, however, completely different to our assumption in H2 (*Sorbus* > *Betula* > *Acer*). There are different possible reasons for this ranking order. Based on Hampel's outlier identification, we identified potential outliers in the value of relative difference of branch volume estimates: *Acer* no. 6 (+10.4%),

Sorbus no. 3 (−35.5%) and *Betula* no. 1 and 5 (−29.1%, −13.2%). Visual inspections of these four point clouds revealed structural shifts within the branches, probably due to registration errors, which significantly decrease the degree of underestimations. The very low R^2_{adj} value of *Acer* can be explained by the impact of the high proportion of large branches as discussed above (i.e., stronger occlusion and larger open contour). Additionally, it could be a result of the very low variability (homogeneity) of the branch volume dimensions: whereas the range was 0.5 to 3.1 dm^3 and 0.7 to 2.0 dm^3 in *Betula* and *Sorbus*, respectively, these values ranged only from 0.5 to 0.7 dm^3 in *Acer*. Both outlier trees of *Betula* tamper with the likely higher mean underestimation of the branches, which otherwise might also be significantly different from *Sorbus*. Branches are most susceptible to thresholds in scan resolution and structural shifts due to movements during the scans or to registration errors. Our results showed that larger branches (diameter at branch center >4 mm) tend to lead to higher means in local overestimations due to additional spatial structures, whereas smaller branches (diameter at branch center <4 mm) will lead to higher means in local underestimation due to a reduction in point densities and insufficient captured small branch structures. Compared with *Betula* the higher R^2_{adj} value for *Sorbus* could also originate in the asymmetry of the crown and therefore a lower degree of occlusion during the scan process.

5. Conclusion

Despite the determined underestimations the results showed that the voxel-based bounding box method provided highly congruent volume estimates based on TLS point clouds. The accuracy of volume estimates primarily depends on the achieved quality of a fully captured tree model. If single young trees are captured with similar high scan resolution the accuracy of total tree wood volume estimates proved to be independent from tree architectural complexity. This is also true for trunk wood volume estimates, a finding that can be related to the fact that trunks constitute the main component of the total wood volume. The impact of occlusions was, thus, not as high as expected for total tree and trunk volume estimates of our sample of single young trees. However, occlusion by branches might be more influential for wood volume estimates of older and larger trees, and for trees scanned within forest stands. In contrast to the total tree and trunk, the accuracy of wood volume estimates for branches significantly differed among tree species and was influenced by tree architectural complexity. This complexity is determined by the number, length and diameter of the branches. However, the degree of estimate accuracy was not related in a simple way to structural complexity, because underestimations originated from different sources in the three tree species: in particular from occlusions and blind spots on stronger branches in *Acer*, and from high numbers of small branches with diameters below scan resolution in *Sorbus* and *Betula*. The accuracy of branch volume estimates can thus not be directly derived from the degree of tree architectural complexity.

As our sample represents a first pool of fully xylometric measured wood volumes, one of our next goals is to further improve TLS-based wood volume estimates of the branches. Considering tree modeling approaches like geometrical cylinder fitting, a combination of voxel-based modeling and cylinder fitting methods referenced to a topological tree model might turn out to complement each other.

Acknowledgments

Author Contributions

Carsten Hess and Goddert von Oheimb conceived and designed the experiment; Carsten Hess did the field and laboratory work; Carsten Hess, Anne Bienert and Werner Härdtle analyzed the data; Carsten Hess, Anne Bienert contributed analysis tools; Carsten Hess, Anne Bienert, Werner Härdtle and Goddert von Oheimb wrote the paper.

Conflicts of Interest

The authors declare no conflict of interest.

References

1. Wagner, S.; Huth, F.; Mohren, F.; Herrmann, I. Silvicultural systems and multiple service forestry. In *Integrative Approaches as an Opportunity for the Conservation of Forest Biodiversity*; Kraus, D., Krumm, F., Eds.; European Forest Institute: Freiburg, German, 2013, pp. 64–73.
2. Wutzler, T.; Wirth, C.; Schumacher, J. Generic biomass functions for Common beech (Fagus sylvatica L.) in Central Europe: Predictions and components of uncertainty. *Can. J. For. Res.* **2008**, *38*, 1661–1675.
3. Kramer, H.; Akça, A. *Leitfaden zur Waldmesslehre*, 5th ed; J. D. Sauerländers Verlag: Frankfurt am Main, Germany, 2008.
4. Zianis, D.; Muukkonen, P.; Makipaa, R.; Mencuccini, M. Biomass and stem volume equations for tree species in Europe. *Silva Fennica Monographs* **2005**, *4*, 1–2, 5–63.
5. Van Breugel, M.; Ransijn, J.; Craven, D.; Bongers, F.; Hall, J.S. Estimating carbon stock in secondary forests: Decisions and uncertainties associated with allometric biomass models. *For. Ecol. Manag.* **2011**, *262*, 1648–1657.
6. Ketterings, Q.M.; Coe, R.; van Noordwijk, M.; Ambagau', Y.; Palm, C.A. Reducing uncertainty in the use of allometric biomass equations for predicting above-ground tree biomass in mixed secondary forests. *For. Ecol. Manag.* **2001**, *146*, 199–209.
7. Kaasalainen, S.; Krooks, A.; Liski, J.; Raumonen, P.; Kaartinen, H.; Kaasalainen, M.; Puttonen, E.; Anttila, K.; Mäkipää, R. Change Detection of Tree Biomass with Terrestrial Laser Scanning and Quantitative Structure Modelling. *Rem. Sens.* **2014**, *6*, 3906–3922.
8. Pretzsch, H. Canopy space filling and tree crown morphology in mixed-species stands compared with monocultures. *For. Ecol. Manag.* **2014**, *327*, 251–264.
9. Fleck, S.; Mölder, I.; Jacob, M.; Gebauer, T.; Jungkunst, H.F.; Leuschner, C. Comparison of conventional eight-point crown projections with LIDAR-based virtual crown projections in a temperate old-growth forest. *Ann. For. Sci.* **2011**, *68*, 1173–1185.

10. Hopkinson, C.; Chasmer, L.E.; Zsigovics, G.; Creed, I.F.; Sitar, M.; Treitz, P.; Maher, R.V. Errors in LiDAR ground elevation and wetland vegetation height estimates. *ISPRS Int. Arch. Photogramm. Rem. Sens. Spat. Inf. Sci.* **2004**, *XXXVI-8/W2*, 108–113.

11. Moskal, L.M.; Zheng, G. Retrieving Forest Inventory Variables with Terrestrial Laser Scanning (TLS) in Urban Heterogeneous Forest. *Rem. Sens.* **2012**, *4*, 1–20.

12. Maas, H.-G.; Bienert, A.; Scheller, S.; Keane, E. Automatic forest inventory parameter determination from terrestrial laser scanner data. *Int. J. Rem. Sens.* **2008**, *29*, 1579–1593.

13. Li, Y.; Hess, C.; von Wehrden, H.; Härdtle, W.; von Oheimb, G. Assessing tree dendrometrics in young regenerating plantations using terrestrial laser scanning. *Ann. For. Sci.* **2014**, *71*, 453–462.

14. Seidel, D.; Beyer, F.; Hertel, D.; Fleck, S.; Leuschner, C. 3D-laser scanning: A non-destructive method for studying above-ground biomass and growth of juvenile trees. *Agr. For. Meteorol.* **2011**, *151*, 1305–1311.

15. Dassot, M.; Colin, A.; Santenoise, P.; Fournier, M.; Constant, T. Terrestrial laser scanning for measuring the solid wood volume, including branches, of adult standing trees in the forest environment. *Comp. Elec. Agr.* **2012**, *89*, 86–93.

16. Bienert, A.; Hess, C.; Maas, H.-G.; von Oheimb, G. A voxel-based technique to estimate the volume of trees from terrestrial laser scanner data. *ISPRS Int. Arch. Photogramm. Rem. Sens. Spat. Inf. Sci.* **2014**, *XL-5*, 101–106.

17. Hackenberg, J.; Morhart, C.; Sheppard, J.; Spiecker, H.; Disney, M. Highly Accurate Tree Models Derived from Terrestrial Laser Scan Data: A Method Description. *Forests* **2014**, *5*, 1069–1105.

18. Vonderach, C.; Vögtle, T.; Adler, P.; Norra, S. Terrestrial laser scanning for estimating urban tree volume and carbon content. *Int. J. Rem. Sens.* **2012**, *33*, 6652–6667.

19. Hosoi, F.; Nakai, Y.; Omasa, K. 3-D voxel-based solid modeling of a broad-leaved tree for accurate volume estimation using portable scanning LIDAR. *ISPRS J. Photogramm. Rem. Sens.* **2013**, *82*, 41–48.

20. Gorte, B.; Winterhalder, D. Reconstruction of Laser-Scanned Trees using Filter Operations in the 3D-Raster Domain. *ISPRS Int. Arch. Photogramm. Rem. Sens. Spat. Inf. Sci.* **2004**, *XXXVI-8/W2*, 39–44.

21. Pfeifer, N.; Gorte, B.; Winterhalder, D. Automatic Reconstruction of Single Trees from Terrestrial Laser Scanner Data. *ISPRS Int. Arch. Photogramm. Rem. Sens. Spat. Inf. Sci.* **2004**, *XXXV Part B5*, 114–119.

22. Raumonen, P.; Kaasalainen, M.; Åkerblom, M.; Kaasalainen, S.; Kaartinen, H.; Vastaranta, M.; Holopainen, M.; Disney, M.; Lewis, P. Fast Automatic Precision Tree Models from Terrestrial Laser Scanner Data. *Rem. Sens.* **2013**, *5*, 491–520.

23. Pueschel, P.; Newnham, G.J.; Rock, G.; Udelhoven, T.; Werner, W.; Hill, J. The influence of scan mode and circle fitting on tree stem detection, stem diameter and volume extraction from terrestrial laser scans. *ISPRS J. Photogramm. Rem. Sens.* **2013**, *77*, 44–56.

24. Liang, X.; Kankare, V.; X.W. Yu; Hyyppa, J.; Holopainen, M. Automated Stem Curve Measurement Using Terrestrial Laser Scanning. *IEEE Trans. Geosci. Remote Sens.* **2014**, *52*, 1739–1748.

25. Astrup, R.; Ducey, M.J.; Granhus, A.; Ritter, T.; von Lüpke, N. Approaches for estimating stand-level volume using terrestrial laser scanning in a single-scan mode. *Can. J. For. Res.* **2014**, *44*, 666–676.

26. Calders, K.; Newnham, G.; Burt, A.; Murphy, S.; Raumonen, P.; Herold, M.; Culvenor, D.; Avitabile, V.; Disney, M.; Armston, J.; *et al.* Nondestructive estimates of above-ground biomass using terrestrial laser scanning. *Meth. Ecol. Evol.* **2015**, *6*, 198–208.

27. Bucksch, A.; Fleck, S. Automated detection of branch dimensions in woody skeletons of leafless fruit tree canopies. *Photogramm. Eng. Rem. Sens.* **2011**, 229–240.

28. Hackenberg, J.; Wassenberg, M.; Spiecker, H.; Sun, D. Non Destructive Method for Biomass Prediction Combining TLS Derived Tree Volume and Wood Density. *Forests* **2015**, *6*, 1274–1300.

29. Pueschel, P. The influence of scanner parameters on the extraction of tree metrics from FARO Photon 120 terrestrial laser scans. *ISPRS J. Photogramm. Rem. Sens.* **2013**, *78*, 58–68.

30. FARO Technologies Inc. *FARO Laser Scanner Photon 20/120*: *User's Manual*, FARO Technologies Inc.: Korntal-Münchingen, Germany, 2010.

31. Team R.C. *R: A Language and Environment for Statistical Computing*; R Foundation for Statistical Computing: Vienna, Austria, 2015.

32. Bucksch, A.; Khoshelham, K. Localized Registration of Point Clouds of Botanic Trees. *IEEE Geosci. Rem. Sens. Lett.* **2013**, *10*, 631–635.

33. Bienert, A.; Maas, H.-G. Methods for the automatic geometric registration of terrestrial laser scanner point clouds in forest stands. *ISPRS Int. Arch. Photogramm. Rem. Sens. Spat. Inf. Sci.* **2009**, *XXXVIII-3/W8*, 93–98.